Journal of Applied Mechanics and Technical Physics, Vol. 43, No. 5, pp. 641–648, 2002

RELAXATION OF A LOW-INTENSITY ATOMIC BEAM IN A QUIESCENT GAS

A. A. Morozov

UDC 533.72:539.188

Relaxation of a low-intensity atomic beam in a gas at rest is examined by means of numerical modeling with the method of test particles. Temperature-field features in the mixing region are considered. A relation between the relaxation length and the initial velocity and mass of injected particles is obtained. Conditions are found under which the relaxation length is minimal.

A numerical study of relaxation of a stationary molecular beam in a gas at rest consists in the calculation and analysis of the parameter fields of injected molecules, which results from beam relaxation from the maximum nonequilibrium at the injection point to diffusive drift at the background-gas temperature. Numerous applied aspects of the problem involve various relaxation stages. The relaxation of the beam governs charge-exchange processes and determines the possibility of extraction of electron or ion beams out of technical apparatus, their purification from neutral particles, and also methods of creating gas-jet obstructing targets [1]. The processes that accompany gas-dynamic separation upon injection of a mixture of gases and isotopes occur at the stage of substantial relaxation of the injected particle flow [2, 3]. In gas-mixing problems related to vacuum technologies, characterization of complete relaxation of an injected gas in a background one is of interest. The mixing of molecular and continuum flows during the interaction of a rocket-engine plume with the ambient high-attitude atmosphere [4], active atmospheric probing with molecular gases or electron beams, electron-beam-assisted plasma production, and sputtering of a target surface with high-energy beams may be considered as belonging to this class of problems.

The problem about the relaxation of a molecular beam was frequently addressed in the following simplest formulation: a unidirectional one-velocity low-intensity beam was considered, and both the collisions of injected particles and their effect on the background gas were ignored. The problem in such a formulation was treated both analytically [5–8] and numerically [9–12].

In the majority of the papers, the following integral characteristics of the relaxation process were examined: depth of penetration of heavy particles into the background gas [8, 9], characteristic time and length of the relaxation zone [5, 10, 11], and variation of the distribution-function moments of injected particles in the course of relaxation [7]. The spatial distribution of gas-dynamic parameters of the injected gas was studied [6, 11]. The formation of high-temperature regions in the relaxation zone during injection of light particles with a high injection velocity was considered [12]. Despite the considerable interest in the molecular-beam relaxation process, no exhaustive description of the phenomenon can be gained from the data obtained.

The present work, devoted to numerical modeling of relaxation of a beam of monoatomic particles in the above formulation, is a continuation of [11]. We consider the special features of the spatial distribution of temperature in the relaxation zone, analyzing simultaneously the distribution of translational energy along different directions in the region with a substantially nonequilibrium state of the gas. Special attention was paid to estimating the relaxation length as a function of the mass and velocity of injected particles using various criteria in a wide range of these parameters.

Kutateladze Institute of Thermal Physics, Siberian Division, Russian Academy of Sciences, Novosibirsk 630090. Translated from Prikladnaya Mekhanika i Tekhnicheskaya Fizika, Vol. 43, No. 5, pp. 3–12, September–October, 2002. Original article submitted January 28, 2002; revision submitted March 15, 2002.

0021-8944/02/4305-0641 $27.00

1. Formulation of the Problem and Main Definitions. We consider the scattering of a unidirectional low-intensity atomic beam on an equilibrium background gas consisting of monoatomic particles. The particles of the beam are injected from a point source. The initial velocities of all atoms in the beam are identical. The collisions of injected particles and their action on the background-gas particles are ignored. The problem is treated using the method of test particles [13].

The spatial motion of particles is traced in a cylindrical volume, with complete absorption of injected particles assumed at its boundary. The direction of the cylinder axis coincides with the injection direction. The dimensions of the cylindrical volume are chosen so that to avoid any appreciable influence of the boundaries on the relaxation zone of injected particles. Considering the problem geometry, we introduce the following cylindrical coordinates: r is the distance to the axis and ε is the azimuth angle, the axis x coincides with the injection direction, and the origin with the position of the source.

To describe the interaction between atoms, we use the hard-sphere model [14]. As a length unit, we use the mean free path of the background-gas particles $\lambda_0 = 1/(n_0\sigma\sqrt{2})$ (n_0 is the number density of the particles and σ is their collision cross-section) and, as velocity and time units, their most probable thermal velocity $c_0 = (2kT_0/m_0)^{1/2}$ (k is the Boltzmann constant, T_0 is the background-gas temperature, and m_0 is the mass of a background-gas particle), and the time $t_0 = \lambda_0/c_0$. From the gained data about the state of injected particles in different parts of the cylindrical volume, the density, velocity, energy, and translational temperature T were calculated. Additionally, we calculate the temperature components $T_\parallel$ and $T_\perp$ parallel and transverse to the velocity vector, respectively, which offers the possibility of analyzing the degree of nonequilibrium along various directions in the relaxation zone. To calculate $T_\parallel$ and $T_\perp$, in each cell we use a local coordinate system (x', r') moving at a velocity equal to that of the gas in the cell: the direction of the x' axis coincides with that of the velocity vector and the r' axis, normal to the x' axis, lies in the xr plane. The temperature components are calculated from the formulas $T_\parallel = m(\langle u_{x'}^2\rangle - \langle u_{x'}\rangle^2)/k$ and $T_\perp = m\langle u_{r'}^2\rangle/k$ [14], where m is the mass of an injected particle and $u_{x'}$ and $u_{r'}$ are the projections of the particle velocity onto the x' and r' axes, respectively.

The numerical experiments were conducted in a wide range of the masses of injected light particles ($M = m/m_0 < 1$) and heavy particles ($M > 1$). The beam velocity was varied from zero to the values two orders of magnitude higher than the thermal velocity of background-gas particles. The ratios between the masses M and velocities $S = u_0/c_0$ (u_0 is the initial velocity of the injected gas) were the problem parameters.

To describe the relaxation zone, we calculated integral characteristics of the process, which were uniquely determined by the parameters S and M. The integral characteristics could be conveniently drawn considering the time evolution of individual particles. To this end, a period during which a particle resided in a volume of interest was divided into intervals of length Δt. To model the motion of the particle at the times $t_1 = \Delta t$, $t_2 = 2\Delta t$, ... , $t_j = j\Delta t$, ... , we determined the axial velocity of the particle u_j, its axial coordinate x_j, and the distance to the injection point $d_j = (x_j^2 + r_j^2)^{1/2}$ (r_j is the radial coordinate). In averaging the quantities over the whole ensemble of injected particles, we calculated the depth of their penetration into the background gas $X_j = \langle x_j\rangle$, the distance to the injection point $D_j = \langle d_j\rangle$, the energy component $(E_x)_j = 0.5m\langle u_j^2\rangle$, and the axial-velocity distribution function $f_j(u)$. As a consequence, for a sufficiently small value of Δt (in the present calculations, this value was $\Delta t = 0.1t_0$), we could reconstruct the time dependences of the above-indicated quantities $X(t)$, $D(t)$, $E_x(t)$, and $f(u, t)$.

For an arbitrary ratio of the masses M, the mean-mass motion of the particles at an infinitely large distance to the source is strictly radial, the same as the motion from some fictitious source with a center at the axis of the cylindrical volume that does not coincide with the injection point. The distance from the fictitious source to the injection point L_s may be used to estimate the length of the relaxation zone [11]. To calculate L_s, we invoke the notion of the penetration depth of injected particles $X(t)$. With increasing t, the dependence $X(t)$ tends to a limiting value $X(\infty)$, which coincides with the distance from the injection point to the fictitious source.

To estimate the distance at which the injected particle "forgets" the direction of its initial motion, we use the notion of the momentum-relaxation length L_i [10, 11]. For each particle, we calculated the axial coordinate x_i at which its axial velocity changed its sign for the first time after the injection (at that moment the particle started moving in the direction opposite to injection). The momentum-relaxation length was calculated as an average value of this coordinate for all test particles: $L_i = \langle x_i\rangle$.

The degree of nonequilibrium of the state of the injected gas could be judged most accurately by comparing between the calculated velocity-distribution function with the equilibrium one at the background-gas temperature. To determine the size of the region with the nonequilibrium state of the gas, we used the notion of the distribution-

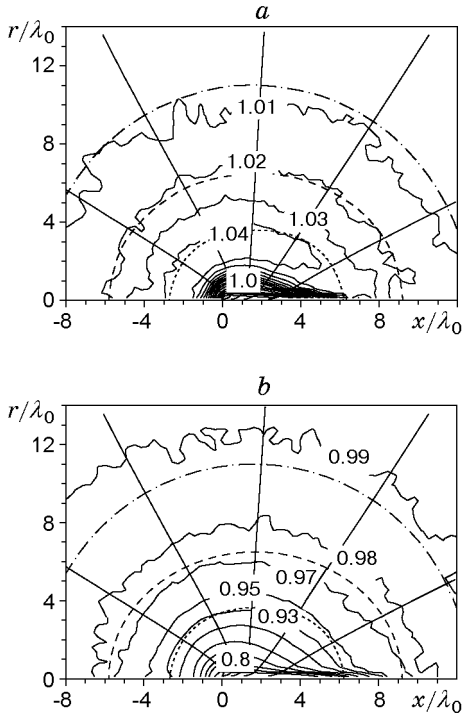

Fig. 1. Streamlines (straight lines) and fields of the temperature components parallel (a) and normal (b) to the local streamline ($M = 1$ and $S = 1$): the dotted, dashed, and dot-and-dashed curves show the relaxation surfaces for the energy, temperature, and temperature components, respectively.

function relaxation length. At certain moments (from the time of particle injection into the gas), we calculated the area of the region bounded by the equilibrium and nonequilibrium distribution functions:

$$\Delta f(t) = \int \max\{0, f_{\rm M}(u) - f(u,t)\}\, du.$$

Here $f_{\rm M}(u) = (c_0\pi^{1/2})^{-1} \exp(-(u/c_0)^2)$ is the Maxwellian distribution function for the thermal-velocity component at the background-gas temperature and $f(u,t)$ is the calculated axial-velocity distribution function of injected particles. The relaxation time of the distribution function was found as an interval between the moment of injection and the time t_f at which the area Δf became smaller than 1% of the total area under the distribution function, i.e., $\Delta f(t_f) = 0.01 \int f_{\rm M}(u)\, du$, and the distribution-function relaxation length L_f was determined as the mean distance from the injection point $D(t_f)$ corresponding to this moment. The calculations show that it took a longer time for the axial velocity to relax compared to the radial velocity; for that reason, the axial velocity component was used to determine the distribution-function relaxation length L_f.

In addition, the characteristic size of the nonequilibrium zone was estimated through a comparison between the energy components of injected and background particles. To this end, for certain moments in time, we calculated the difference between the mean energy $E_x(t)$ and the respective energy of background particles $E_{x0} = 0.25 m_0 c_0^2$. Then, the energy-relaxation time was determined as the interval between the injection moment and the time t_E at which E_x and E_{x0} became identical within 1%, and the energy-relaxation length L_E was determined as the distance $D(t_E)$. It should be noted that the total energy could not be used to calculate the energy-relaxation length since, during injection of heavy particles with certain velocities, the energy of injected and background particles throughout the relaxation remained almost identical, though the injected gas was in an essentially nonequilibrium state and the total energy-relaxation length was equal to zero [11].

To test the program, we performed the above-described calculations for the values of parameters taken from [9, 10]. We calculated the depth of penetration of injected particles into the background gas $X(t)$ [9] and the momentum-relaxation length L_i [10]. The results were found to agree well with the data obtained in [9, 10].

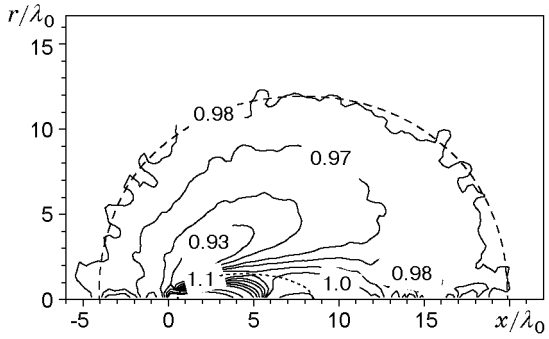

Fig. 2. Temperature field ($M = 10$ and $S = 1$): the dotted curve refers to the surface with the highest temperature and the dashed curve refers to the surface beyond which the temperature and the background-gas temperature are identical within 2%.

2. Spatial Configuration of the Relaxation Zone. The analysis of nonequilibrium in the relaxation zone was performed, based on a comparison between the temperature components determined for different directions. Figure 1 shows the fields of the temperature components parallel ($T_\parallel$) and normal ($T_\perp$) to the local streamline for $M = 1$ and $S = 1$. The isotherms are pear-shaped. The temperature varies from zero at the injection point to the background value at the periphery. The parallel component (Fig. 1a) attains its highest value, $T_\parallel \approx 1.04T_0$, at the surface of an ellipsoid with the semiaxes $4\lambda_0$ and $3\lambda_0$, and then it decreases to the background temperature. The normal component (Fig. 1b) monotonically increases to the background temperature. A comparison between $T_\parallel$ and $T_\perp$ shows that the distribution of particle velocities in different directions may vary appreciably (within an ellipsoid with a characteristic size $R = 4\lambda_0$, the difference between $T_\parallel$ and $T_\perp$ is greater than 10%).

The calculated size of the mixing region depends on the criterion used to determine the relaxation boundary. The energy of injected particles becomes equal to the energy of background particles (within 1%) outside the ellipsoid with a center near a fictitious source ($x_s \approx 1.5\lambda_0$) and a characteristic size $R \approx 4\lambda_0$ (see the dotted curves in Fig. 1). The injected-gas temperature becomes equal to the temperature of background particles (within 1%) only outside the ellipsoid with a characteristic size $R \approx 7\lambda_0$ (dashed curves in Fig. 1), the temperature components on this surface being significantly different: $T_\parallel \approx 1.02T_0$ and $T_\perp \approx 0.975T_0$. Complete relaxation, when the temperatures of the injected and background gases become equal to each other and the velocity distribution of injected particles along different directions becomes isotropic (the values of $T_\parallel$ and $T_\perp$ are identical within 1%), occurs only outside the sphere of radius $R = 11\lambda_0$ (dot-and-dashed curves in Fig. 1).

Determining the integral relaxation length from the trajectories of individual particles (namely, from their axial velocities), we obtain $L_E = 3.46\lambda_0$ and $L_f = 4.03\lambda_0$, which fairly well agrees with the energy-relaxation length obtained from the spatial configuration ($R \approx 4\lambda_0$). Thus, the integral relaxation length is a characteristic size of the region with a nonequilibrium state of the gas at the initial stage of relaxation, whereas the complete-relaxation zone may be much greater.

In varying the value of M or S to either side from unity, the structure of the relaxation zone changes drastically. As the mass ratio M increases, the relaxation zone becomes more elongated in the injection direction. A decrease in the mass ratio M makes the relaxation zone more spherosymmetric. It is of interest to consider how the relaxation zone changes with increasing mass of injected particles.

Figure 2 shows the temperature field for $S = 1$ and $M = 10$. The position of the fictitious source is shifted towards the injection direction; the source lies at the distance $L_f \approx 9.4\lambda_0$ from the source, which corresponds to a strongly anisotropic relaxation zone. Here, a characteristic feature of the temperature field is the nonmonotonic behavior of temperature along the normal to the injection line. The injected gas has an extremely high temperature in a vicinity of a certain surface close to an ellipsoid of revolution with the rotation axis aligned with the injection direction (dotted curve in Fig. 2). The major and minor semiaxes of the ellipsoid are equal to $4\lambda_0$ and $1.5\lambda_0$. Inside the ellipsoid, there is a region with a strongly nonequilibrium state of the gas. In this region, as well as in the case of $M = 1$, the temperature components parallel and normal to the local streamline behave differently. Outside this surface with an elevated temperature, there is a region with a lower temperature. The temperature decreases downstream from its maximum value $1.2T_0$ to $0.9T_0$, and then it gradually increases to the background-gas

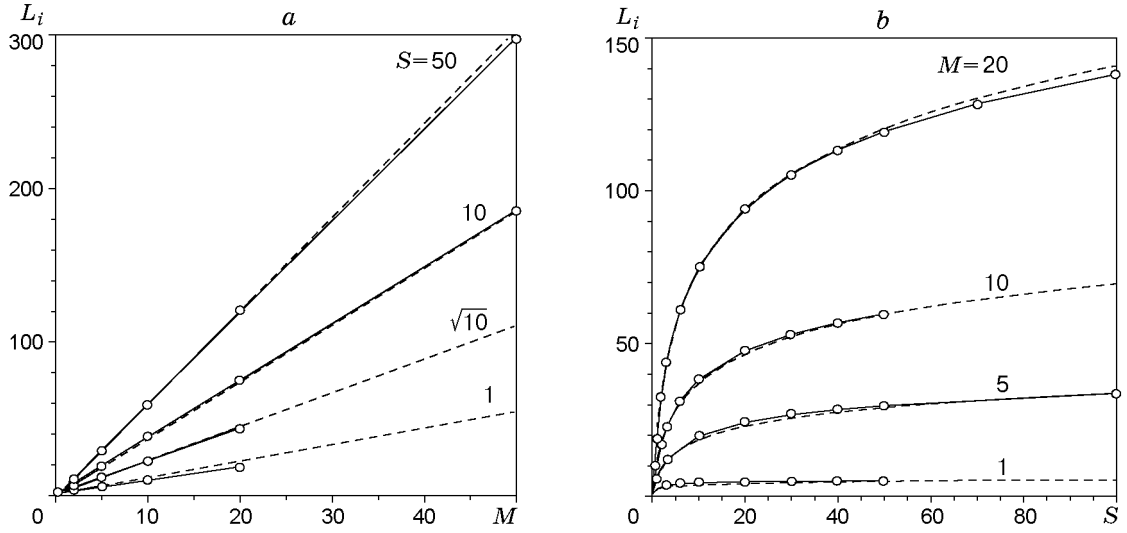

Fig. 3. Momentum-relaxation length L_i versus the mass ratio at a constant initial injection velocity (a) and versus the initial injection velocity at a constant mass ratio (b): the solid curves refer to modeling data and the dashed curves refer to values estimated by formula (3.1).

temperature. The temperature becomes isotropic (the injected-gas and background-gas temperatures are identical within 2%) only outside a spherical surface of radius $12\lambda_0$ with the center at the point $x = 8\lambda_0$ (dashed curve in Fig. 2).

3. Integral Characteristics of the Process. A study of the relaxation kinetics of an atomic beam allows one to obtain sufficiently full information about the integral characteristics and, in particular, to obtain more accurate relevant data compared to [10, 11].

The relation between the momentum-relaxation length and the mass and velocity ratios is rather trivial (Fig. 3). Based on the calculated values, we made an attempt to fit these dependences with a sufficiently simple function. In the range of the mass ratio $1 \leqslant M \leqslant 20$ and velocity ratio $2 \leqslant S \leqslant 50$, the fitting function found is

$$L_i(M, S) = (1.55M - 0.8) \ln [(S + 1)(10M + 3)/(10M - 9)]. \tag{3.1}$$

Figure 3 compares the momentum-relaxation length obtained by numerical simulation with that predicted by formula (3.1). Here, we consider the dependence of L_i on the mass at fixed values of the initial injection velocity $S = 1$, $\sqrt{10}$, 10, and 50 (Fig. 3a) and on the initial injection velocity at fixed masses $M = 1$, 5, 10, and 20 (Fig. 3b). It is seen that, with an increase in M and S, the difference between the calculated values and the values predicted by formula (3.1) increases.

The behavior of the energy-relaxation length and that of the distribution-function relaxation length are more intricate. Figures 4 and 5 show, respectively, the above-indicated quantities as functions of the mass ratio at fixed injection velocities $S = 0.5$, 1, $\sqrt{10}$, and 10 and as functions of the initial injection velocity at fixed mass ratios $M = 0.05$, 0.1, 1, and 10. It is seen that there is a clear correlation between the two lengths.

At a fixed velocity ratio S and $M \to 0$ and $M \to \infty$, the relaxation length L increases indefinitely (see Fig. 4). At all values of the velocity ratio, the quantity L attains a minimum at $M = 1$, which corresponds to a more rapid relaxation in the case of identical masses of particles. Besides, if particles are injected with a high initial velocity ($S > 1$), a second minimum of L appears at such a mass ratio $M_{\min}$ at which the initial injected-gas energy $E_{\min}$ is 20% lower than the background-gas energy $E_0 = 0.75 m_0 c_0^2$. For instance, for $S = \sqrt{10}$, we have $M_{\min} = 0.12$ and $E_{\min} = 0.8E_0$ (see Fig. 4c), and for $S = 10$, we have $M_{\min} = 0.012$ and $E_{\min} = 0.8E_0$ (see Fig. 4d).

At a fixed mass ratio M and $S \to \infty$, the relaxation length L increases (see Fig. 5). As $S \to 0$, the value of L saturates at a certain non-zero level. For heavy particles ($M > 1$), as the ratio S increases, a monotonic growth of the relaxation length is observed, whereas the dependence of the relaxation length for light particles ($M < 1$) displays a minimum. The minimum relaxation length $L_{\min}$ is attained at such an initial injection velocity $S_{\min}$ at which the initial injected-gas energy $E_{\min}$ is approximately 30% lower than the background-gas energy E_0. For instance, for $M = 0.05$, we have $S_{\min} = 4.5$ and $E_{\min} = 0.67E_0$ (see Fig. 5a), whereas for $M = 0.1$, we have $S_{\min} = 3.3$ and $E_{\min} = 0.73E_0$ (see Fig. 5b).

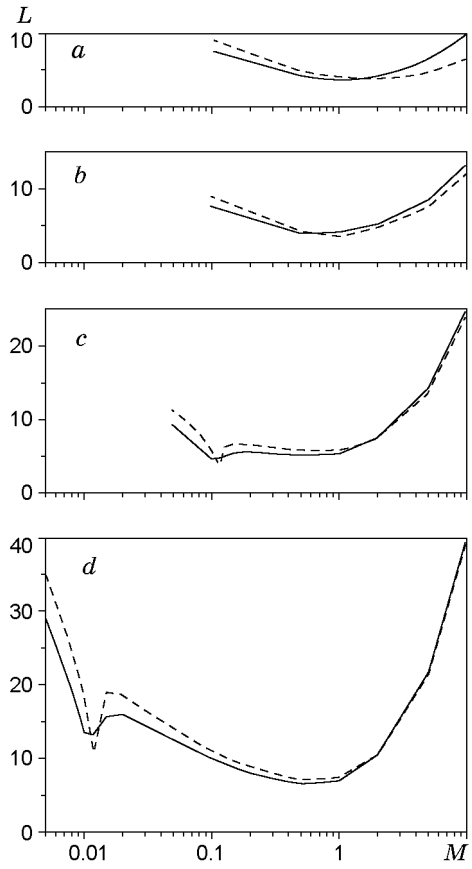

Fig. 4

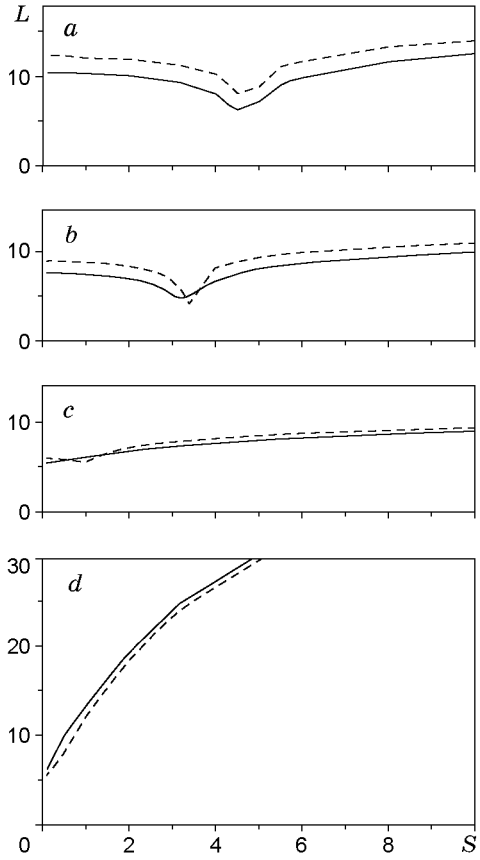

Fig. 5

Fig. 4. Distribution-function relaxation length L_f (solid curves) and energy-relaxation length L_E (dashed curves) versus mass relation for $S = 0.5$ (a), 1 (b), $\sqrt{10}$ (c), and 10 (d).

Fig. 5. Distribution-function relaxation length L_f (solid curves) and energy-relaxation length L_E (dashed curves) versus the initial velocity for $M = 0.05$ (a), 0.1 (b), 1 (c), and 10 (d).

The occurrence of the minimum point at $M < 1$ can be explained by the fact that, during the collisions with heavy particles, the light particles rapidly lose the directed velocity, with redistribution of translational energy among the three velocity components. If the initial energy of injected light particles differs considerably from the energy of background-gas particles, then, after several collisions, the injected particles acquire a Maxwellian velocity distribution with a temperature different from the background-gas value. In subsequent collisions with background particles, there will be further exchange by energy between the injected and background-gas particles, and the injected-gas temperature will gradually approach the background-gas value. Since the masses of injected and background-gas particles differ considerably, the energy exchange in each collision is insignificant, and the relaxation process is long. If the initial energy of injected particles is close to the energy of background-gas particles, then, already after several first collisions and redistribution of the initial energy, the injected particles will have an equilibrium distribution with a temperature close to the background-gas value. Thus, during injection of light particles with an energy close to the energy of background-gas particles, the relaxation process will be substantially accelerated. The evolution of the distribution function $f(u, t)$ of the particle velocity parallel to the injection axis shown in Fig. 6 for $M = 0.1$ and the initial velocities $S = 2$, $\sqrt{10}$, and 6 at the times $t = t_0$, $2t_0$, and $3t_0$ provides a support for this explanation. For $MS^2 = 1$ and $S = \sqrt{10}$ ($E = 0.67E_0$), the distribution function for the particle velocity already at $t = 3t_0$ differs from the equilibrium velocity-distribution function for the background-gas temperature by no more than 1%. For $S = 2$ and 6 ($E = 0.27E_0$ and $2.4E_0$), the distribution functions at the same moment are close to Maxwellian ones but have a temperature respectively lower and higher

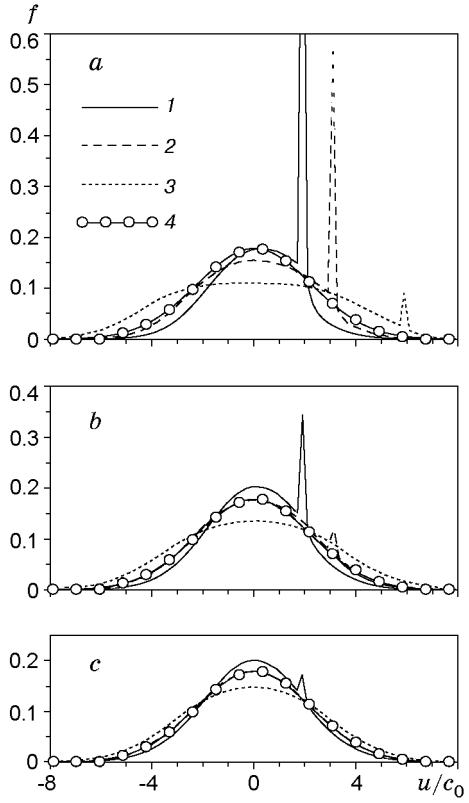

Fig. 6. Evolution of the velocity-distribution function $f(u,t)$ of injected particles for the velocity parallel to the injection axis ($M = 0.1$) for $t = t_0$ (a), $2t_0$ (b), and $3t_0$ (c); curves 1, 2, and 3 refer to $S = 2$, $\sqrt{10}$, and 6, respectively; curve 4 is the Maxwellian distribution for the background-gas temperature.

than the background-gas temperature ($T \approx 0.8T_0$ and $1.4T_0$), the relaxation time ($7t_0$ and $7.5t_0$) being much more longer than for $S = \sqrt{10}$ ($3t_0$). The relaxation lengths for the velocity ratios under consideration are $7\lambda_0$, $4.7\lambda_0$, and $8.6\lambda_0$ (see Fig. 5b), i.e., the length decreases approximately by 40% at the minimum point.

It should be noted that the above effects do not depend on the criterion used to determine the relaxation length. Above, this length was determined using, as such a criterion, attainment of a 1% difference between the energies or distribution functions of injected and background-gas particles. With the relaxation length determined from the condition that the above differences equal 0.5 or 2%, although the relaxation length changes slightly, the $L(M)$ and $L(S)$ dependences still behave similarly.

From the comparative analysis of the momentum-relaxation length, energy-relaxation length, and the distance from the injection point to the fictitious source, the following conclusions can be drawn. In the considered range of mass and velocity ratios, the distance between the injection point and the fictitious source is somewhat greater than the momentum-relaxation length (approximately by $0.6\lambda_0$). The energy-relaxation length is always greater than the momentum-relaxation length. For heavy particles, this difference ranges between one and six mean free paths. For light particles with $M \to 0$, the energy-relaxation length increases, whereas the momentum-relaxation length tends to a certain value equal to the mean free path for the given velocity S. For heavy particles, the energy-relaxation length and the velocity-distribution function relaxation length acquire almost identical values; hence, during injection of heavy particles ($M > 1$), any of the above-considered characteristics (L_i, L_E, L_f, or L_s) may be used to estimate the relaxation-zone length.

Conclusions. Based on direct modeling with the method of test particles, the present study of the kinetics of relaxation of an atomic beam in a gas at rest has revealed qualitative and quantitative relaxation characteristics for atomic-beam relaxation to thermal equilibrium with the background gas within the range of the mass ratio of injected and background-gas particles 0.005–50 and within the range of their velocity ratio 0.1–100 (with atoms modeled as hard spheres). The conclusions drawn from the qualitative analysis also remain valid for a wider range of these parameters.

A formula is obtained which relates the momentum-relaxation length with the mass and velocity ratios M and S in the ranges $1 \leqslant M \leqslant 20$ and $2 \leqslant S \leqslant 50$. A relation is found between the energy-relaxation length and the velocity distribution function relaxation length, and the mass ratio and initial injection velocity. This relation is not monotonic for the most part, with minima occurring at $MS^2 \sim 1$. It is found that, during injection of heavy particles ($M > 1$), any of the considered characteristics (L_i, L_E, L_f, or L_s) may be used to estimate the length of the relaxation zone. The data obtained permit estimation of the length of the nonequilibrium mixing zone of injected and background gases at a low intensity of the atomic beam.

The author thanks Dr. A. K. Rebrov and M. Yu. Plotnikov for the problem statement and help in the work.

This work was supported by the Presidium of the Russian Academy of Sciences (6th Competition-Expertize of Young Scientists' Research Projects, Russian Acad. of Sci., 1999), Grant No. 57.

REFERENCES

1. V. P. Ivanov, "Gas-dynamic purification of an ion beam from neutral molecules," *Zh. Tekh. Fiz.*, **44**, No. 2, 380–386 (1974).
2. Yu. S. Kusner, S. S. Kutateladze, V. G. Prikhod'ko, et al., "Inertial gas-dynamic separation of gas mixtures and isotopes," *Dokl. Akad. Nauk SSSR*, **247**, No. 4, 845–848 (1979).
3. R. G. Gallagher and J. B. Anderson, "Isotope separation in crossed-jet systems," in: *11th Int. Symp. on Rarefied Gas Dynamics*, Vol. 1, Paris (1979), pp. 629–637.
4. G. A. Luk'yanov, "Scattering of hypersonic flow on a supersonic gas jet in a free-molecular interaction regime," *Izv. Akad. Nauk SSSR, Mekh. Zhidk. Gaza*, No. 1, 176–179 (1973).
5. B. I. Khripunov, "Relaxation of neutral-particle beams in a gas," *Zh. Tekh. Fiz.*, **48**, No. 9, 1890–1897 (1978).
6. S. F. Chekmarev, "Scattering of a beam of heavy noninteracting particles on a light gas," in: *Diagnostics of Rarefied Gas Flows* (collected scientific papers) [in Russian], Inst. of Thermal Physics, Sib. Div., Acad. of Sci. of the USSR, Novosibirsk (1979), pp. 189–195.
7. V. C. Boffi and G. Spiga, "Exact time-dependent solutions to the nonlinear Boltzmann equation," in: *15th Int. Symp. on Rarefied Gas Dynamics* (Grado, Italy, June 16–20, 1986), Vol. 1, B. G. Teubner, Stuttgart (1986), pp. 55–63.
8. P. Riesco-Chueca, R. Fernandez-Feria, and J. Fernandez de la Mora, "Interspecies transfer of momentum and energy in disparate mass gas," *Phys. Fluids*, **30**, No. 1, 45–55 (1987).
9. J. B. Anderson, "Low energy particle range," *J. Chem. Phys.*, **63**, No. 4, 1504–1512 (1975).
10. B. L. Paklin and A. K. Rebrov, "Interaction of molecular flow from a point source with a continuous medium," *J. Appl. Mech. Tech. Phys.*, **36**, No. 5, 643–646 (1995).
11. A. A. Morozov, M. Yu. Plotnikov, and A. K. Rebrov, "Kinetics of degradation of a molecular beam in a gas at rest," *J. Appl. Mech. Tech. Phys.*, **38**, No. 4. 590–597 (1997).
12. A. A. Morozov, M. Yu. Plotnikov, and A. K. Rebrov, "Shock effects accompanying degradation of a molecular beam," *Tech. Phys. Lett.*, **23**, No. 9, 663–664 (1997).
13. M. Perlmutter, "Solution of problems about the Couette flow and heat transfer between parallel plates in a rarefied gas using the Monte Carlo method," in: *Numerical Methods in Rarefied Gas Dynamics* [Russian translation], Mir, Moscow (1969), pp. 116–139.
14. G. Bird, *Molecular Gas Dynamics*, Clarendon Press, Oxford (1976).